Green emitting polyhedral oligomeric silsesquioxanes/ poly(phenylene vinylene) derivative materials for highly efficient organic light emitting diodes (OLEDs)

C.W. Lee[1,2], Y. Josse[1], C.H. Hsu[2], and T.P. Nguyen[1,a]

[1] Institut des Matériaux Jean Rouxel, Université de Nantes, 2 rue de la Houssinière, BP 32229, 44322 Nantes, France
[2] Department of Applied Chemistry, National Chiao Tung University, Hsinchu 30010, Taiwan, Republic of China

Abstract. Hybrid materials composed of polyhedral oligomeric silsesquioxanes (POSS) and a polyphenylene vinylene (PPV) derivative were fabricated and characterized by optical and surface spectroscopy. The hybrid thin films have similar optical properties as the pristine polymer but contributions of the POSS are evidenced in infrared spectroscopy. Organic light emitting diodes using the hybrid material as an emitter clearly showed an improvement of the electrical characteristics and the efficiency of the devices as compared to those using the pristine polymer. The effects of POSS incorporation to the polymer are discussed via the obtained results.

PACS. 78.60.Fi Electroluminescence – 72.80.Le Polymers; organic compounds – 78.30.Am Elemental semiconductors and insulators – 72.80.Tm Composite materials

1 Introduction

Conjugated polymers have been extensively studied for their applications in electroluminescence devices since the first report on organic light-emitting diodes (OLEDs) [1]. For the applications of devices, the two most important requirements are a high emission efficiency and a thermal stability of the organic material. Among the many conjugated polymers that have been used as an emitter in devices, poly(1,4-phenylenevinylene) (PPV) and their derivatives have attracted a great attention in recent years because of their high stability and their good electroluminescence [2–6].

Hsieh et al. have proposed a synthetic route to poly(2,3-diphenyl-1,4-phenylenevinylene) ($DPOC_{10}$-PPV) which exhibits a high photoluminescence efficiency in the solid state [7]. By using this route, a high molecular weight and soluble $DPOC_{10}$-PPV was obtained. Different substituents were then introduced to the polymer structure to improve its properties [8,9]. However, the performance of devices using $DPOC_{10}$-PPV polymers is still not high enough to employ them in displays. It is possible that the regular hexagonal structures of the main chain form strong π–π interactions and, hence, reduce the electroluminescence efficiency [10].

Polyhedral oligomeric silsesquioxanes (POSS) are new organic-inorganic hybrid materials of high interest for electronic devices because of their ability to link with conjugated polymer chains to tune the band gap and, hence, the light emission of the materials [11–16]. POSS materials are composed of a silica block, which is surrounded by organic substitution groups. The incorporation of bulky POSS in a polymer host matrix can reduce significantly the aggregation of chains and can improve the quality of the emission, avoiding formation of low energy sites such as excimers and exciplexes. Furthermore, as POSS contains inorganic blocks, the hybrid organic-inorganic polymers are less sensitive to oxidation and thermal effects than the corresponding pristine polymer. As a matter of fact, devices using such materials usually exhibit significant improvement in stability and performance as compared to conjugated polymers alone.

In this study, we have investigated hybrid materials using a $DPOC_{10}$-PPV derivative attached to a POSS centre core. We characterized the hybrid films by optical and surface measurements and we compared the results to those obtained in pristine polymer films. The films were used as emitting layers in OLEDs and the optoelectronic performances of the diodes were measured and compared to those using only the polymer. We discussed the effects of POSS existence in the polymer chains on the performance of devices.

[a] e-mail: nguyen@cnrs-imn.fr
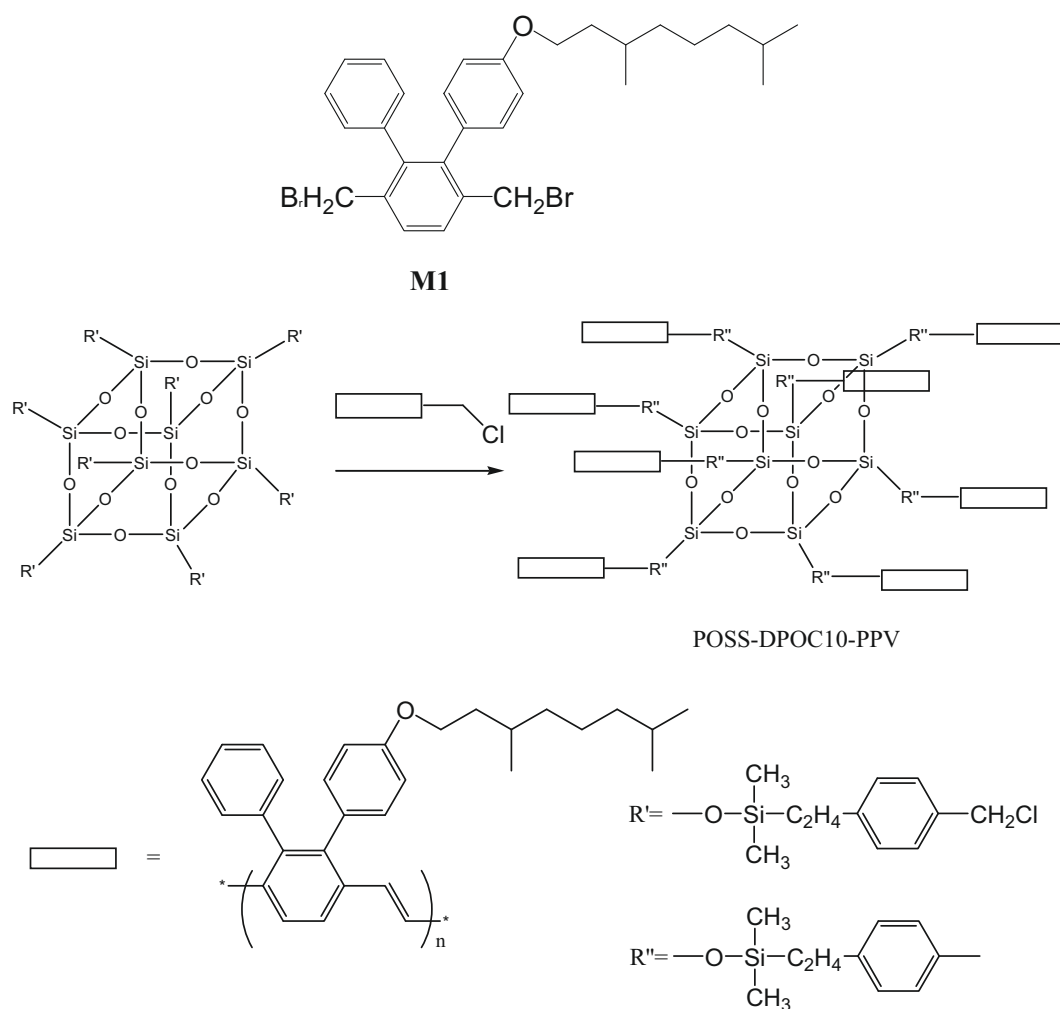
Fig. 1. Structure of monomer M1 and synthesis of POSS-(DPOC$_{10}$-PPV).

2 Experimental

All reagents and chemicals were purchased from commercial sources (Aldrich, Merck, Lancaster) and used without further purification. Tetrahydrofuran (THF) and dichloromethane (CH$_2$Cl$_2$) were dried by distillation using sodium/benzophenone and calcium hydride, respectively. The synthetic routes for monomer M1 were prepared following the method previously described in the literature [17]. The PPV derivative, poly[2-(4′-(3,7-dimethyloctoxy)phenyl)-3-phenyl]-1,4-phenylenevinylene or DPOC$_{10}$-PPV, was then synthesized as follows. A mixture of POSSCHCl (8.4 mg, 0.0038 mmole), and 1,4-bis(chloromethyl)-2-[4′-(3,7-dimethyloctoxy)phenyl]-3-phenyl benzene (0.3 g, 0.62 mmole) were dissolved in anhydrous THF. Then potassium tert-butoxide (0.84 g, 7.49 mmole) dissolved in 22 ml anhydrous THF was added to the solution, which was stirred for 7 h in room temperature. Next, 2,6-di-tert-butylphenol (0.5 g, 2.42 mmole) dissolved in anhydrous 5 ml THF was added and the obtained solution was stirred for 7 h. A yellow solid (0.15 g) was obtained after re-precipitation using

methanol. Figure 1 shows the structure of the monomer and the synthesis of POSS-(DPOC$_{10}$-PPV).

The POSS-(DPOC$_{10}$-PPV) powder was dried at 60 °C under vacuum for 24 h then dissolved in toluene with concentration of 10 mg/ml. Single-layer devices were fabricated as sandwich structures between calcium (Ca) cathodes and indium tin oxide (ITO) anodes. ITO-coated glass substrates were cleaned sequentially in ultrasonic baths of detergent, 2-propanol/deionized water (1:1 volume) mixture, toluene, de-ionized water and acetone. A 50 nm-thick hole injection layer of poly(ethylenedioxythiophene) (PEDOT) doped with poly (styrenesulfonate) (PSS) was spin-coated on top of ITO substrates from a 0.7 wt % dispersion in water and was dried at 150 °C for 1 h in vacuum. Thin films of synthesized polymer of thickness of 50 nm, were spin-coated from toluene solutions onto the PEDOT layer and were dried at 50 °C overnight in vacuum. Finally, 35 nm Ca and 100 nm Al electrodes were deposited through a shadow mask onto the polymer films by thermal evaporation, using an Auto 306 vacuum coater (BOC Edwards, Wilmington, MA). The evaporations were carried out typically at base pressures lower than 8×10^{-7} mbar. The active area of the devices was 4 mm^2.
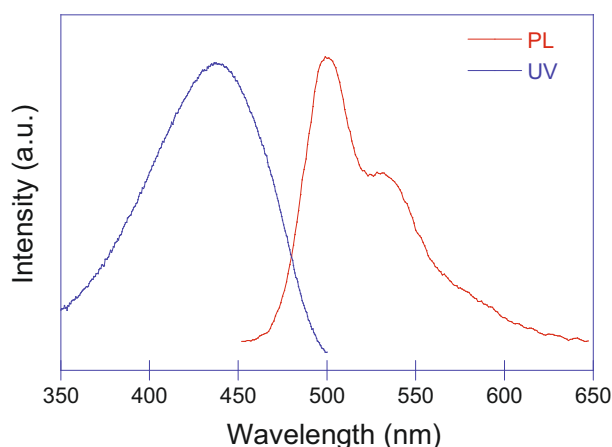
Fig. 2. Absorption and emission spectra of POSS-(DPOC$_{10}$-PPV) thin films.

UV-vis absorption spectra of the samples were measured with a Cary 5G spectrophotometer and photoluminescence (PL) spectra were obtained with a Fluorolog Horiba spectrophotometer. FT-IR and Raman experiments were performed by using a Bruker Vertex 70 and a Bruker RFS 100 spectrophotometer respectively. All the measurements were performed at room temperature.

Cyclic voltammetry (CV) measurements of the polymers were carried out in acetonitrile (CH$_3$CN) with 0.1 M tetrabutylammonium hexafluorophosphate (TBAPF$_6$) at ambient temperature under nitrogen gas with a scan rate of 50 mV/s. Platinum wires were used for both the counter and the working electrodes, and silver/silver ions (Ag in 0.1 M AgNO$_3$ solution, from Bioanalytical Systems, Inc.) were used as the reference electrode, and ferrocene as the standard of oxidation. The polymer film was drop-casted on the Pt working electrode.

3 Results and discussion

3.1 Characterization of hybrid thin films

Figure 2 shows the absorption and the emission spectra of hybrid thin films at room temperature. The maximum of the absorption peak is observed at 435 nm, corresponding to the π–π^* transitions along the conjugated backbone of the polymer. The photoluminescence (PL) spectrum exhibits a maximum at 500 nm and a shoulder at 533 nm. The shape of the PL spectrum is similar to that obtained in PPV [18] and the energy separation between contributions is approximately 150 meV, which is consistent with phonon replica in PPV. These spectra are similar to those obtained in pristine polymer films, and no blue shift of the emission spectrum has occurred. The blue shift of the PL spectrum has been observed in some POSS/oligomer hybrid materials [19] and is assigned to the chain separation by POSS units, reducing the energy transfer between the oligomer chains. However, in several other systems as in our materials (POSS/polymer), such a shift is not produced [20,21], which suggests that the effect of the POSS

Table 1. Assignments for the FT-IR bands of POSS-(DPOC$_{10}$-PPV) thin films.

Wavenumber (cm^{-1})	Assignments	Ref.
700	C-H bending out of plane of phenyl group	[22]
756	CH$_2$ rock	[23]
828	Symmetric out of plane C-H wag	[23]
913	Trans-vinylene out of plane CH bending	[24]
968	Vinylene C-H wag	[25]
1026	Si-O-Si stretching	[22]
1109	Si-O-Si stretching	[26]
1175	Phenyl-oxygen stretching	[27]
1242	C-O-C stretching	[22]
1285	C-H bending in plane of phenyl group	[22]
1382	Symmetric alkyl CH$_2$	[25]
1417	Semicircular phenyl stretching	[25]
1469	Antisymmetric alkyl CH$_2$	[25]
1512	Paraphenylene semicircle stretch	[28]
1574	C=C stretching of the phenyl group	[22]
1609	C=C stretching of the phenyl group	[23]
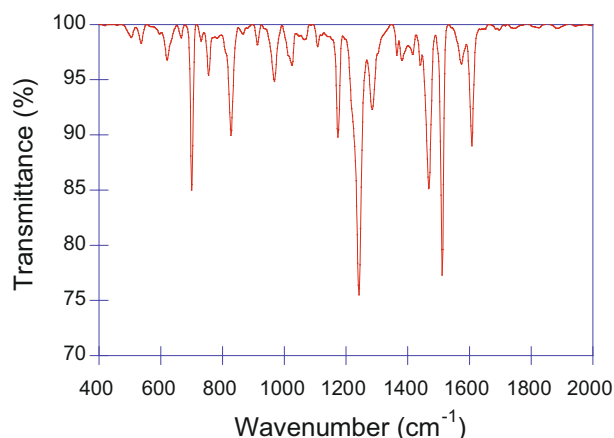
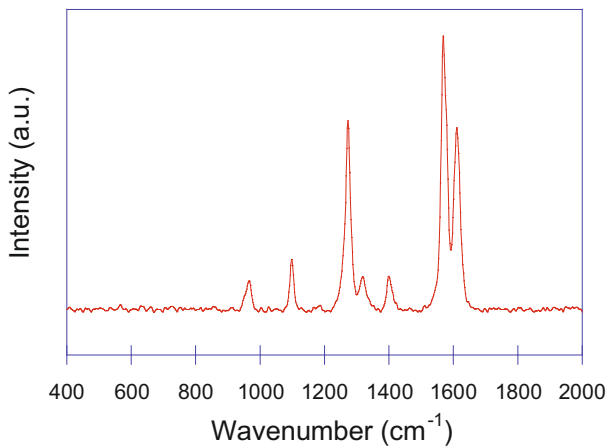**Fig. 3.** IR spectrum of POSS-(DPOC$_{10}$-PPV) thin films.

units on the chain aggregation is negligible. It is possible that the structure of oligomers could favour their separation by POSS units while that of polymer does not, due to their large size.

Table 1 lists the main vibrational modes, which are observed in the IR spectrum shown in Figure 2. The two characteristic silicon peaks (Si-O-Si stretching) correspond to POSS units in the hybrid polymer. The intensity of these peaks is weak because the concentration of POSS is lower than that of polymer. The Raman spectrum of the hybrid films is shown in Figure 3, and Table 2 displays the corresponding peaks. All the observed peaks are assigned to the polymer, and no vibrational bands of Si could have been retrieved.

In order to obtain information on the charge injection from the electrodes, cyclic voltammetry was performed on the synthesized hybrid material and Figure 5 shows the cyclic voltammogram of POSS-(DPOC$_{10}$-PPV). The

**Table 2.** Assignments for the Raman bands of POSS-(DPOC$_{10}$-PPV) thin films.

Wavenumber	Assignments	Ref.
(cm^{-1})		
964	Torsion of CH trans vinylene out of plane	[24]
1097	Symmetric CH$_2$-O-CH$_2$ stretch	[23]
1271	Inter-ring stretching mode	[29]
1317	Elongation of C=C transvinyl	[24]
1398	Elongation of symmetrical hexant cycle	[24]
1567	C=C stretching of the phenyl group	[30]
1609	Intra-ring C-C stretching mode	[29]

Fig. 4. Raman spectrum of POSS-(DPOC$_{10}$-PPV) thin films.
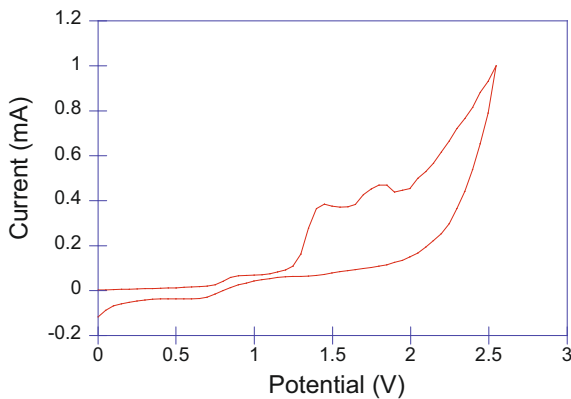
Fig. 5. Cyclic voltammogram of POSS-(DPOC$_{10}$-PPV) film.

HOMO energy level is determined from the onset of the oxidation curve, which is given by:

$$\text{HOMO(eV)} = -\left| E_{ox} + 4.4 \right|. \qquad (1)$$

The HOMO level of POSS-(DPOC$_{10}$-PPV) is -5.5 eV, which is reproducible with fresh polymer films. Its optical band gap energy (E_g) was determined from the absorption edge of the UV-vis spectrum, which is 485 nm and corresponds to a band gap of 2.56 eV. The LUMO level of POSS-(DPOC$_{10}$-PPV) was obtained from the difference between HOMO energy level and the electrical band gap
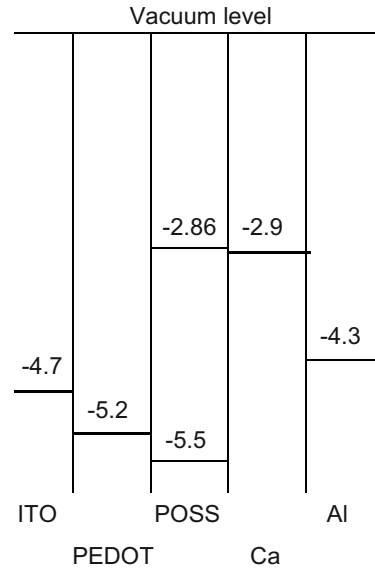
Fig. 6. Band diagram for ITO/PEDOT/ POSS-(DPOC$_{10}$-PPV)/Ca/Al light emitting diodes.

energy. The latter is determined from the optical band gap and the exciton energy, which is $1240/500 = 2.48$ eV. The value of the LUMO is -2.86 eV. The energy level diagram of the ITO/PEDOT/ POSS-(DPOC$_{10}$-PPV)/Ca/Al devices is tentatively proposed in Figure 6.

The characterization results show that incorporation of POSS to the polymer leaves unchanged the properties of the host matrix. The electronic structure of the polymer is not affected by the oxide units as observed in several other hybrid systems [31].

3.2 Device characterization

To test the performance of the hybrid materials, we have realized organic light-emitting diodes of single layer structure ITO/PEDOT/ POSS-(DPOC$_{10}$-PPV)/Ca/Al. After that, an UV curing epoxy adhesive was used in N$_2$ atmosphere for the encapsulation. The electroluminescent (EL) spectrum of the devices is similar to the PL spectrum, indicating that the light emission originates from the polymer chains. From the band diagram, the potential barrier is determined to be 0.3 eV at the anode and 0.04 eV at the cathode. The current-voltage and luminance characteristics of the diode are plotted in Figure 7. Compared to devices using the pristine polymer [17], the I-V characteristic is shifted to higher voltages, with a turn-on voltage of $V_{to} = 8$ V. However, the maximum of luminance in the hybrid devices is higher, reaching 930 cd/m^2 (compared to only 303 cd/m^2 in pristine DPOC$_{10}$-PPV based diodes). On the other hand, the maximum yield of the devices (Fig. 8) using the POSS-(DPOC$_{10}$-PPV) hybrid (1.2 cd/A) is also better than that of the polymer based diodes (0.69 cd/A).

The performance of diodes using the POSS-(DPOC$_{10}$-PPV) is obviously improved as compared to devices using the pristine polymer. Previous investigations of POSS
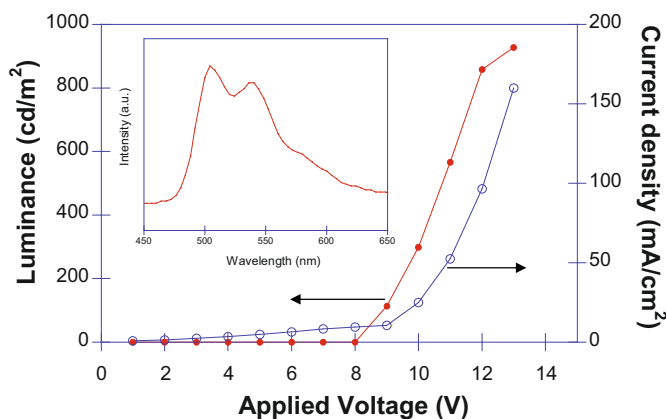
Fig. 7. Current-Voltage-Luminance characteristic of a ITO/PEDOT/POSS-(DPOC$_{10}$-PPV)/Ca/Al diode at $T = 300$ K. Inset: electroluminescence spectrum of the diode.
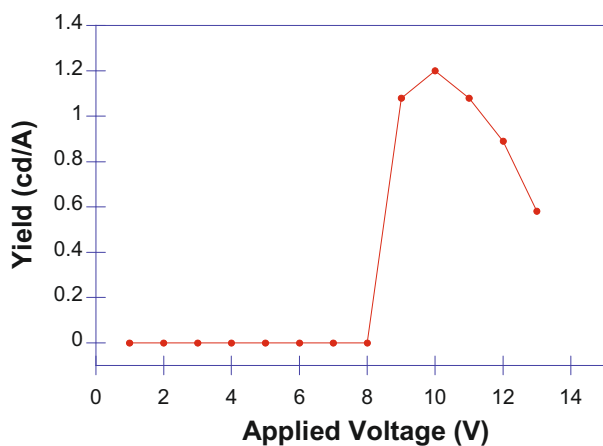
Fig. 8. Yield-voltage curve for the device of a ITO/PEDOT/POSS-(DPOC$_{10}$-PPV)/Ca/Al diode at $T = 300$ K.

based diodes have suggested the improvement of the light emission would be due to the fact that POSS units separate the polymer chains, and reducing aggregation effects [31–33]. However, such a process would imply a blue shift of the PL spectrum in POSS-polymer hybrid material, which is not observed in our samples. Therefore, the effects of the POSS incorporation on the chain aggregation are negligible in the devices studied. Improvements in recombination process in OLEDs may also result from a more balanced transport of holes and electrons in devices. In fact, in most polymers, holes are more mobile than electrons and the difference in the charge carrier transport reduces the recombination possibility, leading to poor device efficiency. Optimized charge balance by modifying the carrier mobility in the polymer would improve the performance of the diodes. As DPOC$_{10}$-PPV is a hole type polymer, the transport balance indicates that the POSS units act as hole blockers or hole trapping centers, reducing their mobility and favouring the recombinations with electrons. This explanation is in agreement with the current-voltage characteristics of the devices using POSS-polymer hybrid material. We observe that the current in

these diodes is lower than that obtained in devices using the pristine polymer for a given applied voltage [17]. The turn-on voltage is enhanced (8V) as compared to that obtained in devices using the pristine polymer (6V). In contrast, the yield is higher when POSS units are incorporated (1.2 compared to 0.69 cd/A). This low intensity can be indicative of carrier trapping processes [35]. Finally, because of the deposition process of thin films, the POSS units can accumulate on the top layer, forming small insulating areas near the PEDOT layer and modify the hole injection. Such a process would result in an increase of the light emission accompanied by a decrease in the current intensity of the device. Further microscopy work on the interface between the hybrid films and the anode will be helpful in understanding the formation and distribution of the POSS units in the polymer matrix (underway).

4 Conclusion

We have investigated a hybrid material made by incorporating POSS star-like material to a PPV derivative, which emits a green light. Optical and surface characterizations of the hybrid thin films showed that POSS units do not affect significantly the electronic properties of the polymer structure. Single-layer devices using the material as an active layer showed an increase of the performance as compared to those using the pristine polymer despite a decrease in electrical conductivity. We explain the obtained results by the balance of the charge transport in the polymer, resulting from a hole trapping process by POSS units that can further block these carriers at the anode and cause a decrease in the current intensity.

References

1. J.H. Burroughes, D.D.C. Bradley, A.R. Brown, R.N. Marks, K. Mackay, R.H. Friend, P.L. Burn, A.B. Holmes, Nature (London) **347**, 539 (1990)
2. D. Braun, A.J. Heeger, Appl. Phys. Lett. **58**, 1982 (1991)
3. H. Spreitzer, H. Becker, E. Kluge, W. Kreuder, H. Schenk, R. Demandt, H. Schoo, Adv. Mater. **10**, 1340 (1998)
4. F. Liang, Y.J. Pu, T. Kurata, J. Kido, H. Nishide, Polymer **46**, 3767 (2005)
5. B.H. Sohn, K. Kim, D.S. Choi, Y.K. Kim, S.C. Jeoung, J.I. Jin, Macromolecules **35**, 2876 (2002)
6. S.H. Jin, M.Y. Kim, J.Y. Kim, K. Lee, Y.S. Gal, J. Am. Chem. Soc. **126**, 2474 (2004)
7. W.C. Wan, H. Antoniadis, V.E. Choong, H. Razafitrimo, Y. Gao, W.A. Field, B.R. Hsieh, Macromolecules **30**, 6567 (1997)
8. B.R. Hsieh, Y. Yu, E.W. Forsythe, G.M. Schaaf, W.A. Feld, J. Am. Chem. Soc. **120**, 231 (1998)
9. S.H. Yang, J.T. Chen, A.K. Li, C.H. Huang, K.B. Chen, B.R. Hsieh, C.S. Hsu, Thin Solid Films **477**, 73 (2005)
10. Y.C. Li, K.B. Chen, H.L. Chen, C.S Hsu, C.S. Tsao, J.H. Chen, S.A. Chen, Langmuir **22**, 11009 (2006)
11. J. Lee, H.J. Cho, B.J. Jung, N.S. Cho, H.K. Shim, Macromolecules **37**, 8523 (2004)

12. J.M. Kang, H.J. Cho, J. Lee, J.I. Lee, S.K. Lee, N.S. Cho, D.H. Hwang, H.K. Shim, Macromolecules **39**, 4999 (2006)
13. K.B. Chen, H.Y. Chen, S.H. Yang, C.S. Hsu, J. Polym. Res. **13**, 237 (2006)
14. S. Xiao, M. Nguyen, X. Gong, Y. Cao, H. Wu, D. Moses, A.J. Heeger, Adv. Funct. Mater. **13**, 25 (2003)
15. X. Gong, C. Soci, C. Yang, A.J. Heeger, S. Xiao, J. Phys. D: Appl. Phys. **39**, 2048 (2006)
16. R.H. Lee, H.H. Lai, Eur. Polym. J. **43**, 715 (2007)
17. K.B. Chen, H.C. Li, C.K. Chen, S.H. Yang, B.R. Hsieh, C.S. Hsu, Macromolecules **38**, 8617 (2005)
18. F.A.C. Oliveira, L.A. Cury, A. Righi, R.L. Moreira, P.S.S. Guimaraes, F.M. Matinaga, M.A. Pimenta, R.A. Nogueira, J. Chem. Phys. **119**, 9777 (2003)
19. K.B. Chen, Y.P. Chang, S.H. Yang, C.S. Hsu, Thin Solid Films **514**, 103 (2006)
20. K.Y. Pu, B. Zhang, Z. Ma, P. Wang, X.Y. Qi, R.F. Chen, L.H. Wang, Q.L. Fan, W. Huang, Polymer **47**, 1970 (2006)
21. J. Lee, H.J. Cho, N.S. Cho, D.H. Hwang, H.K. Shim, Synthetic Metals **156**, 590 (2006)
22. G. Socrates, *Infrared and Raman Characteristic Group Frequencies Tables and Charts* (John Wiley & Sons, Chichester, 2001)
23. A. Mabrouk, S. Ayachi, B. Zaidi, J.P. Buisson, P. Molinié, K. Alimi, Eur. Polym. J. **39**, 2121 (2003)
24. K. Alimi, P. Molinié, M. Majdou, J.C. Bernede, J.L. Fave, H. Bouchriha, M. Ghedira, Eur. Polym. J. **37**, 781 (2001)
25. J.C. Scott, J.H. Kaufman, P.J. Brock, R. DiPietro, J. Salem, J.A. Goitia, J. Appl. Phys. **79**, 2745 (1996)
26. J. Mu, Y. Liu, S. Zheng, Polymer **48**, 1176 (2007)
27. R.K. Khillan, Y. Su, K. Varahramyan, Thin Solid Films **483**, 416 (2005)
28. L.J. Rothberg, M. Yan, M.E. Galvin, E.W. Kwock, T.M. Miller, F. Papadimitrakopoulos, Synthetic Metals **80**, 41 (1996)
29. E. Mulazzi, A. Ripamonti, L. Athouël, J. Wery, S. Lefrant, Phys. Rev. B **65**, 085204 (2002)
30. E. Mulazzi, A. Ripamonti, J. Wery, B. Dulieu, S. Lefrant, Phys. Rev. B **60** 16519 (1999)
31. W.J. Lin, W.C. Chen, W.C. Wu, Y.H. Niu, A.K.Y. Jen, Macromolecules **37**, 2335 (2004)
32. C.H. Chou, S.L. Hsu, K. Dinakaran, M.Y. Chiu, K.H. Wei, Macromolecules **38**, 745 (2005)
33. H.J. Cho, D.H. Hwang, J.I. Lee, Y.K. Jung, J.H. Park, J. Lee, S.K. Lee, H.K. Shim, Chem. Mater. **18**, 3780 (2006)
34. W.P. Chang, W.T. Whang, Polymer **37**, 4227 (1996)
35. C. Renaud, C.H. Huang, M. Zemmouri, P. Le Rendu, T.P. Nguyen, Eur. J. Appl. Phys. **36**, 215 (2007)